Supplementary Information

ABHD12 and LPCAT3 interplay regulates a lyso-phosphatidylserine-C20:4 phosphatidylserine lipid network implicated in neurological disease

Taka-Aki Ichu †, Alex Reed†, Daisuke Ogasawara†, Olesya Ulanovskaya‡, Amanda Roberts§, Carlos A. Aguirre§, Liron Bar-Peled†⊥, Jie Gao||, Jason Germain†, Sabrina Barbas†, Kim Masuda†, Bruno Conti§, Peter Tontonoz||, and Benjamin F. Cravatt†*

† Department of Chemistry, The Scripps Research Institute, La Jolla, CA, USA

‡ Lundbeck, La Jolla, CA, USA

§ Department of Molecular Medicine, The Scripps Research Institute, La Jolla, CA, USA

|| Pathology and Laboratory Medicine, University of California Los Angeles, Los Angeles, CA, USA

*To whom correspondence should be addressed: cravatt@scripps.edu

Supplementary Figures and Tables

Table S1. Complete lipidomic data for human THP-1 cells and mouse brain tissue.

See accompanying Excel file.

Tab	Tab name	Description	Related to
1	MRM list	List of MRM transitions used to perform lipidomic experiments	All lipidomic data
2	LC-MS conditions	LC-MS conditions used to collect lipidomic data	All lipidomic data
3	LPCAT3-KO THP-1 + DO264	Lipid measurement in LPCAT3-deficient THP-1 cells treated with DO264	Figure 1, Figure S2, Figure S3, and Figure S4
4	N-LPCAT3-KO + DO264	Lipid measurement in N-LPCAT3 (–/–) mice treated with DO264	Figure 2 and Figure S5
5	11-week-old double-KO	Lipid measurement in 11-week-old WT, ABHD12 (–/–), N-LPCAT3 (–/–) and double-KO mice	Figure 3, Figure S6, Figure S7, and Figure S8
6	9-month-old double-KO	Lipid measurement in 9-month-old WT, ABHD12 (–/–), N-LPCAT3 (–/–) and double-KO mice	
7	Nestin-Cre metabolomics	Basal lipid measurements in nestin-Cre mice	

Table S2. Genotypic ratios obtained for generating N-LPCAT3(–/–) mice and ABHD12/N-LPCAT3 double-KO mice.

Genotypic ratios obtained from LPCAT3(fl/fl) and LPCAT3 (fl/fl) nestin-Cre intercrosses.

Genotype	Number of mice	Observed (%)	Expected (%)
LPCAT3 (fl/fl)	84	52	50
LPCAT3 (fl/fl) nestin-Cre	77	48	50

Genotypic ratios of mice obtained from ABHD12(+/–)/ LPCAT3 (fl/fl) and ABHD12(+/–)/ LPCAT3 (fl/fl) nestin-Cre intercrosses. There was no statistically significant difference between the observed and expected frequencies (P = 0.31 by Chi-square test).

Genotype			Number of mice	Observed (%)	Expected (%)
ABHD12	LPCAT3	Nestin Cre			
WT	fl/fl	-	49	13.0	12.5
WT	fl/fl	Cre	44	11.6	12.5
KO	fl/fl	-	61	16.1	12.5
KO	fl/fl	Cre	47	12.4	12.5
Het	fl/fl	-	83	22.0	25.0
Het	fl/fl	Cre	94	24.9	25.0

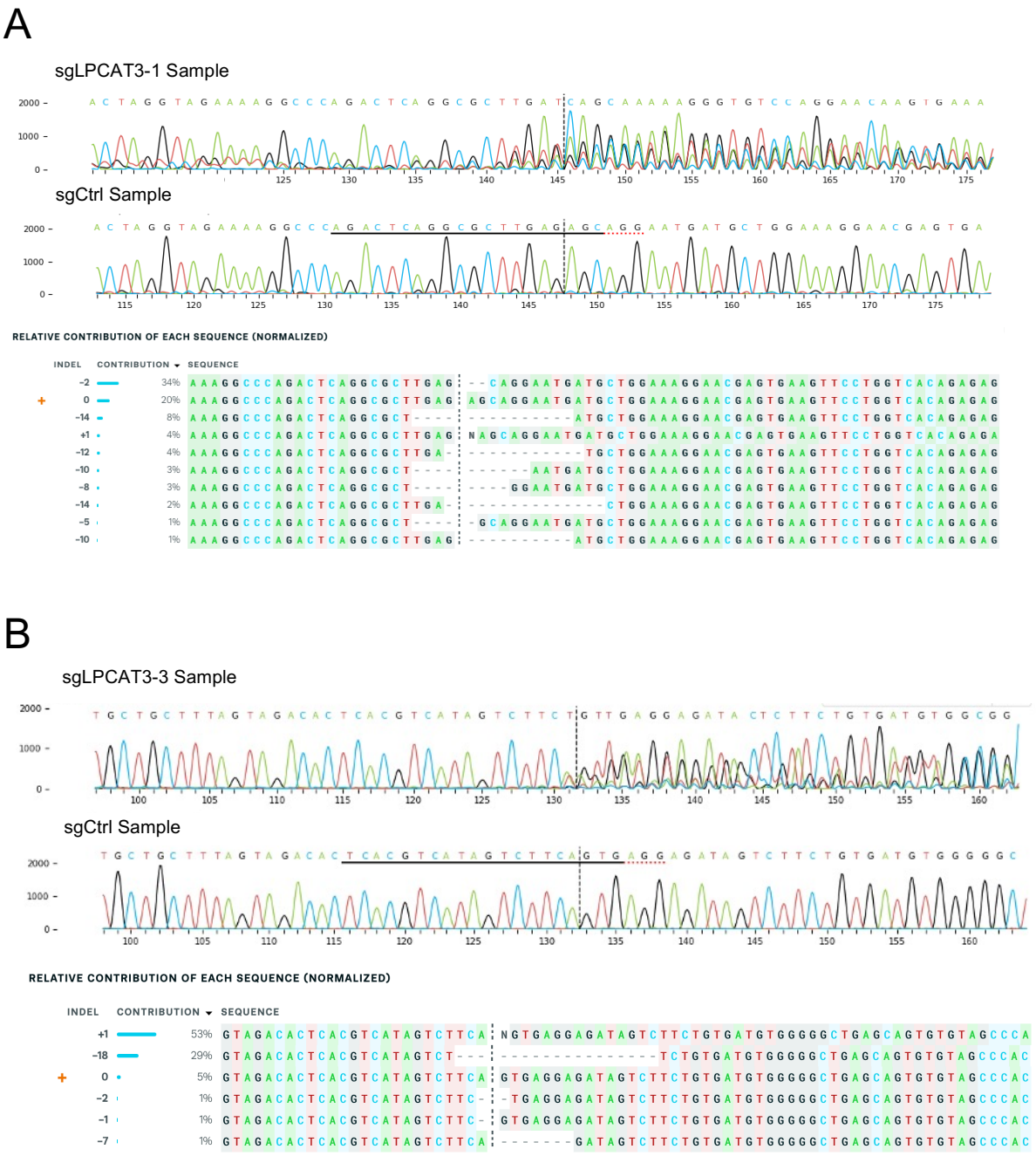

Figure S1. Sequencing validation of representative LPCAT3-deficient THP-1 cells generated by the CRISPR/Cas9 system. Genomic DNA flanking the LPCAT3 CRISPR-Cas9 cut sites was PCR-amplified and subjected to Sanger sequencing. Sequencing tracks from the non-targeting control sgRNA (sgCtrl) and sgRNA targeting LPCAT3 (sgLPCAT3-1 and sgLPCAT3-3, A and B respectively) were aligned using the ICE software.

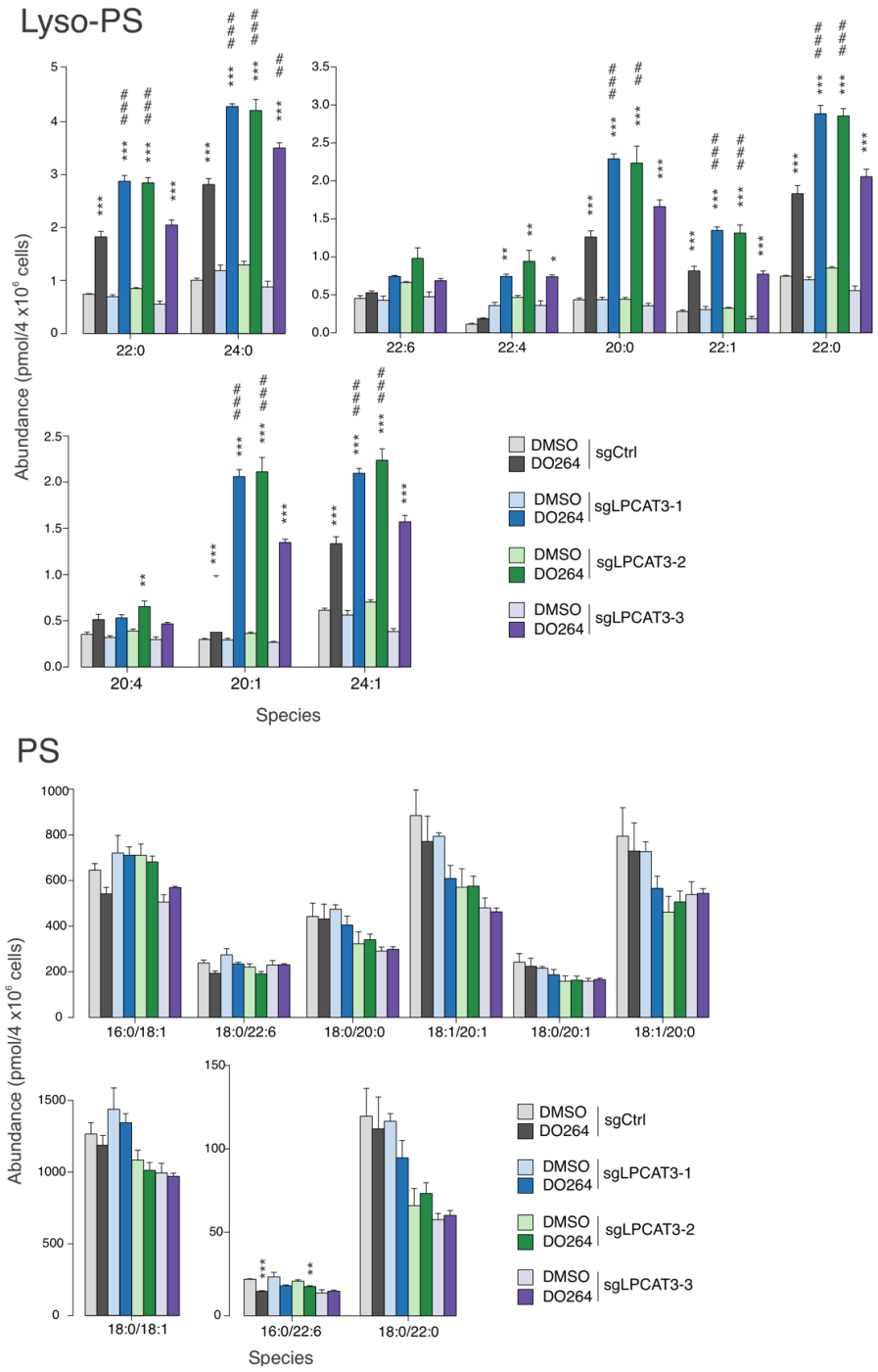

Figure S2. Additional lyso-PS and PS profiles of LPCAT3-deficient THP-1 cells. Related to **Figure 1**. Data represent mean ± SE values. n = 3/group. *P < 0.05; **P < 0.01; ***P < 0.001, two-sided Student's t-test performed relative to DMSO control among each cell line.

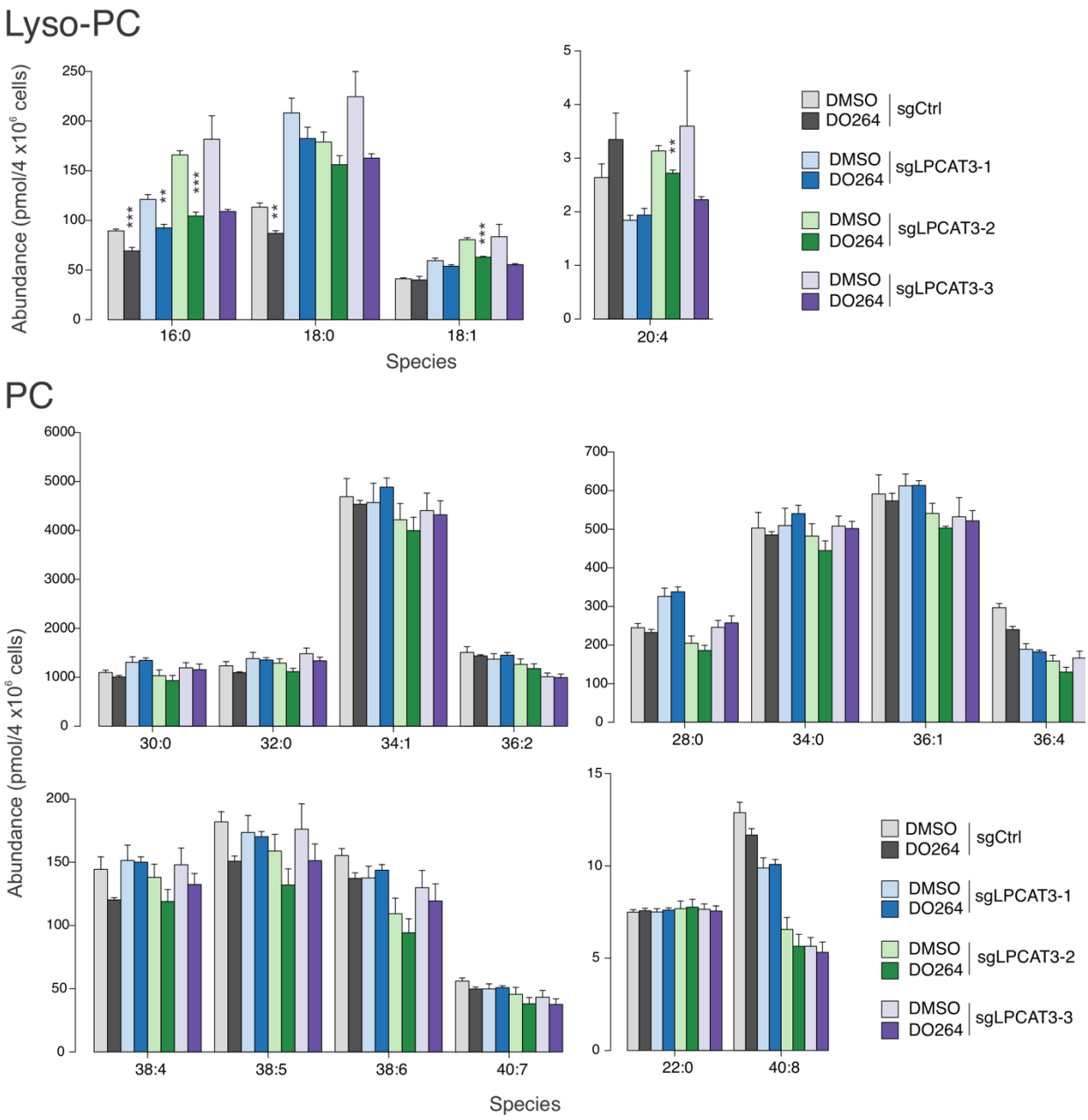

Figure S3. Lyso-PC and PC profiles of LPCAT3-deficient THP-1 cells treated with DO264. Related to **Figure 1**. Data represent mean ± SE values. n = 5/group. *P < 0.05; **P < 0.01; ***P < 0.001, two-sided Student's t-test performed relative to DMSO control among each cell line.

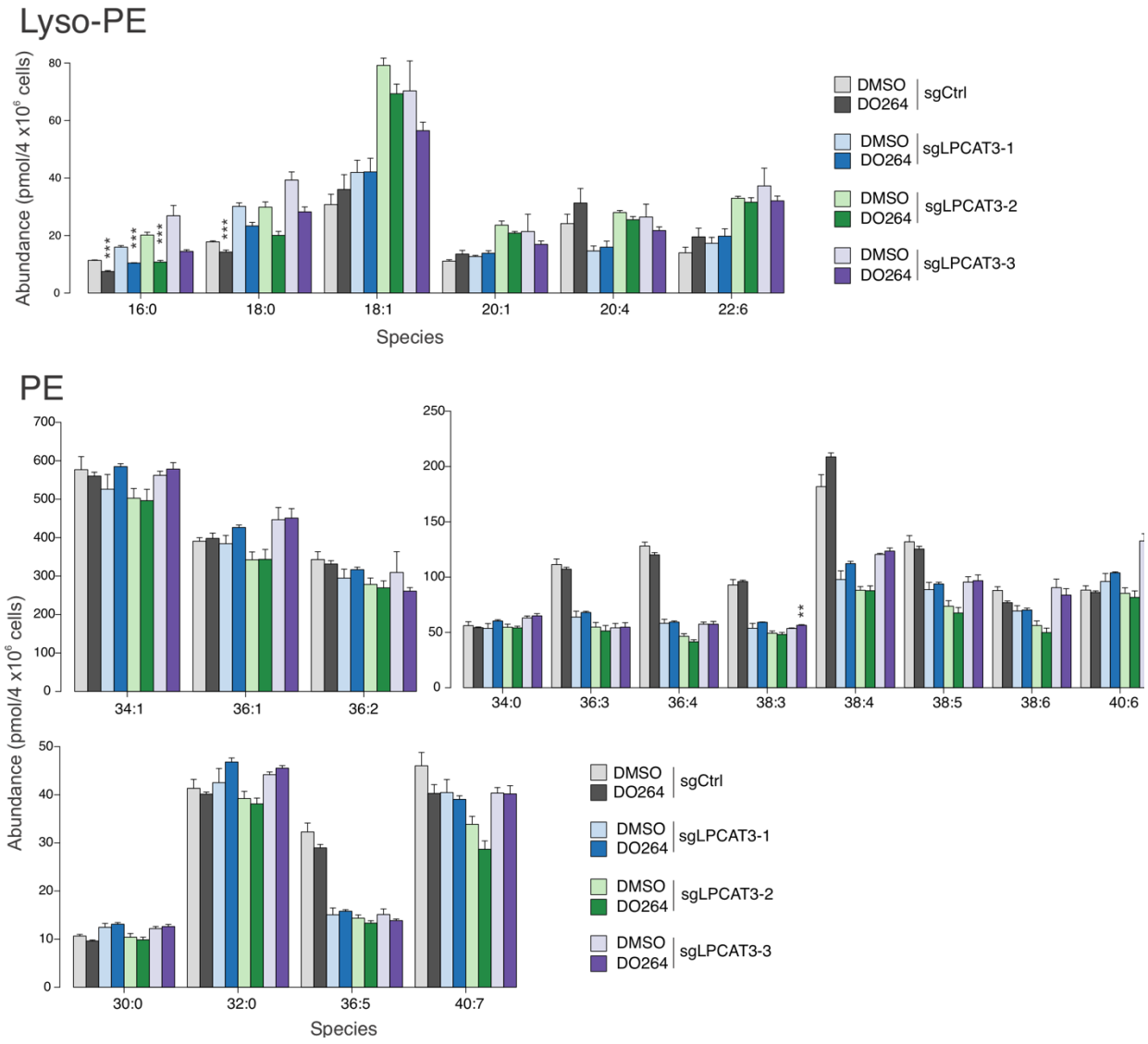

Figure S4. Lyso-PE and PE profiles of LPCAT3-deficient THP-1 cells treated with DO264. Related to **Figure 1**. Data represent mean ± SE values. n = 3/group. *P < 0.05; **P < 0.01; ***P < 0.001, two-sided Student's t-test performed relative to DMSO control among each cell line.

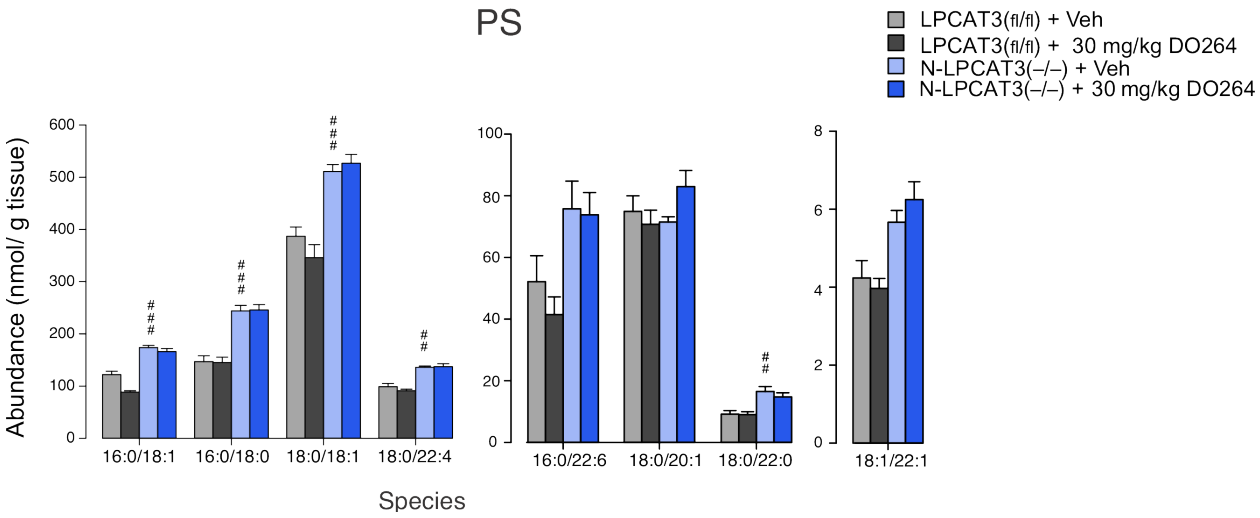

Figure S5. Additional PS profile of DO264-treated N-LPCAT3(–/–) mice. Related to **Figure 2**. Data represent mean ± SE values. n = 5/group. * or # $P < 0.05$; ** or ## $P < 0.01$; *** or ### $P < 0.001$. Asterisks (*) were used for LPCAT3(fl/fl) + Veh vs LPCAT3(fl/fl) + 30 mg/kg DO264 and N-LPCAT3(–/–) + Veh vs N-LPCAT3(–/–) + 30 mg/kg DO264 comparisons. Pounds (#) were used for LPCAT3(fl/fl) + Veh vs N-LPCAT3(–/–) + Veh comparisons.

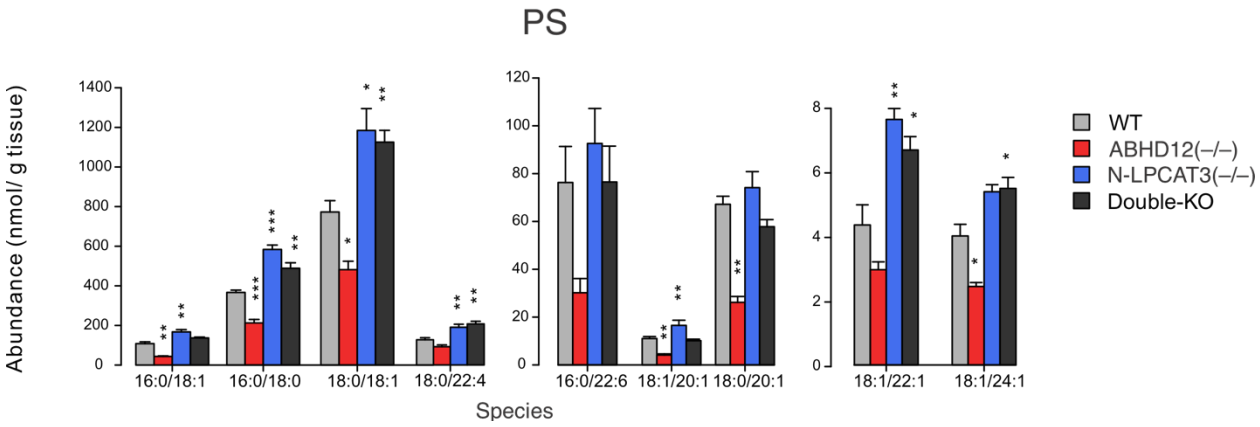

Figure S6. Additional PS profiles of 11-week-old WT, ABHD12(–/–), N-LPCAT3(–/–), and double-KO mice. Related to **Figure 3**. Data represent mean ± SE values. n = 5/group. *P < 0.05; **P < 0.01; ***P < 0.001, two-sided Student's t-test performed relative to WT.

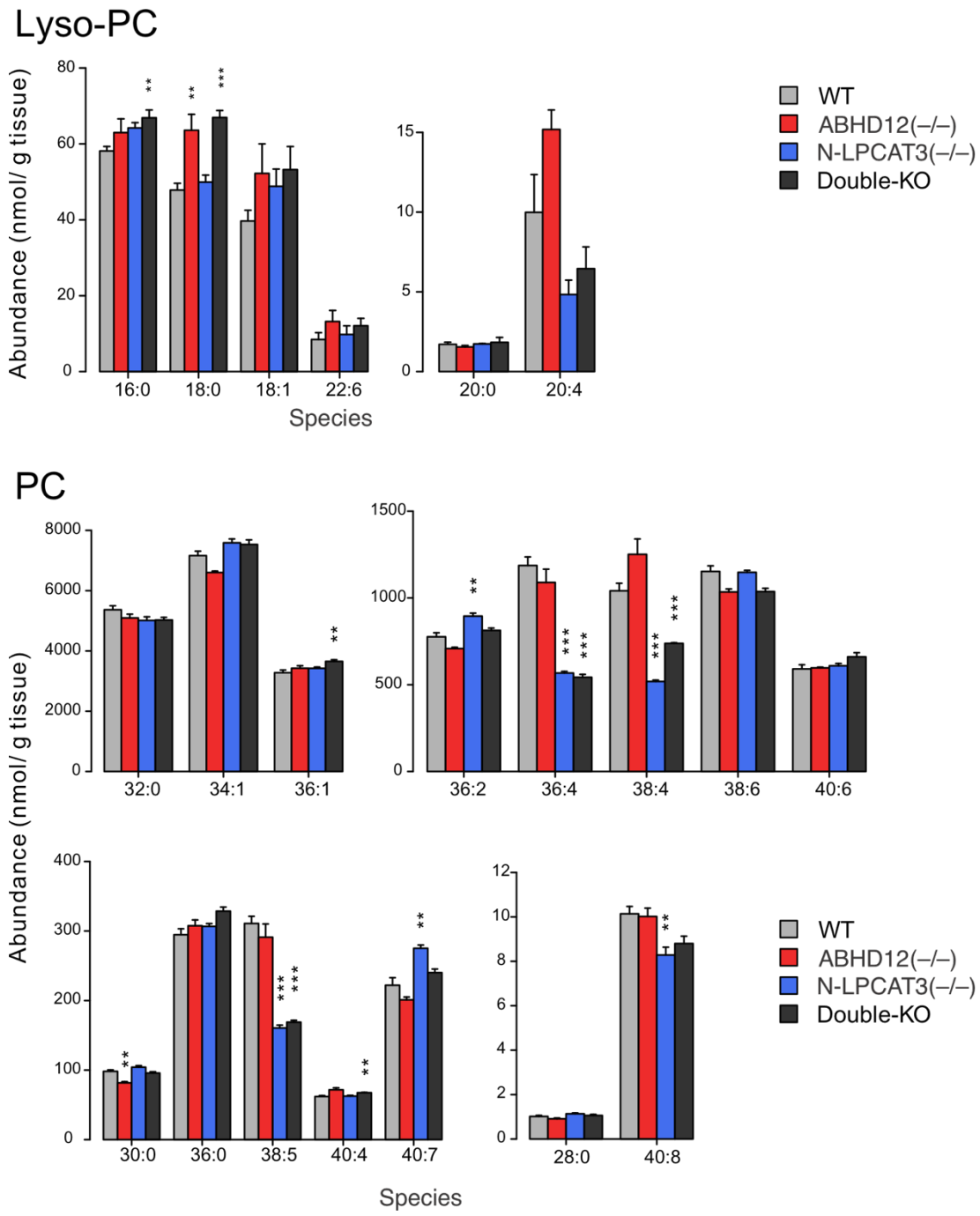

Figure S7. Lyso-PC and PC profiles of 11-week-old ABHD12/N-LPCAT3 double-KO mice. Related to **Figure 3**. Data represent mean ± SE values. n = 5/group. *P < 0.05; **P < 0.01; ***P < 0.001, two-sided Student's t-test performed relative to WT.

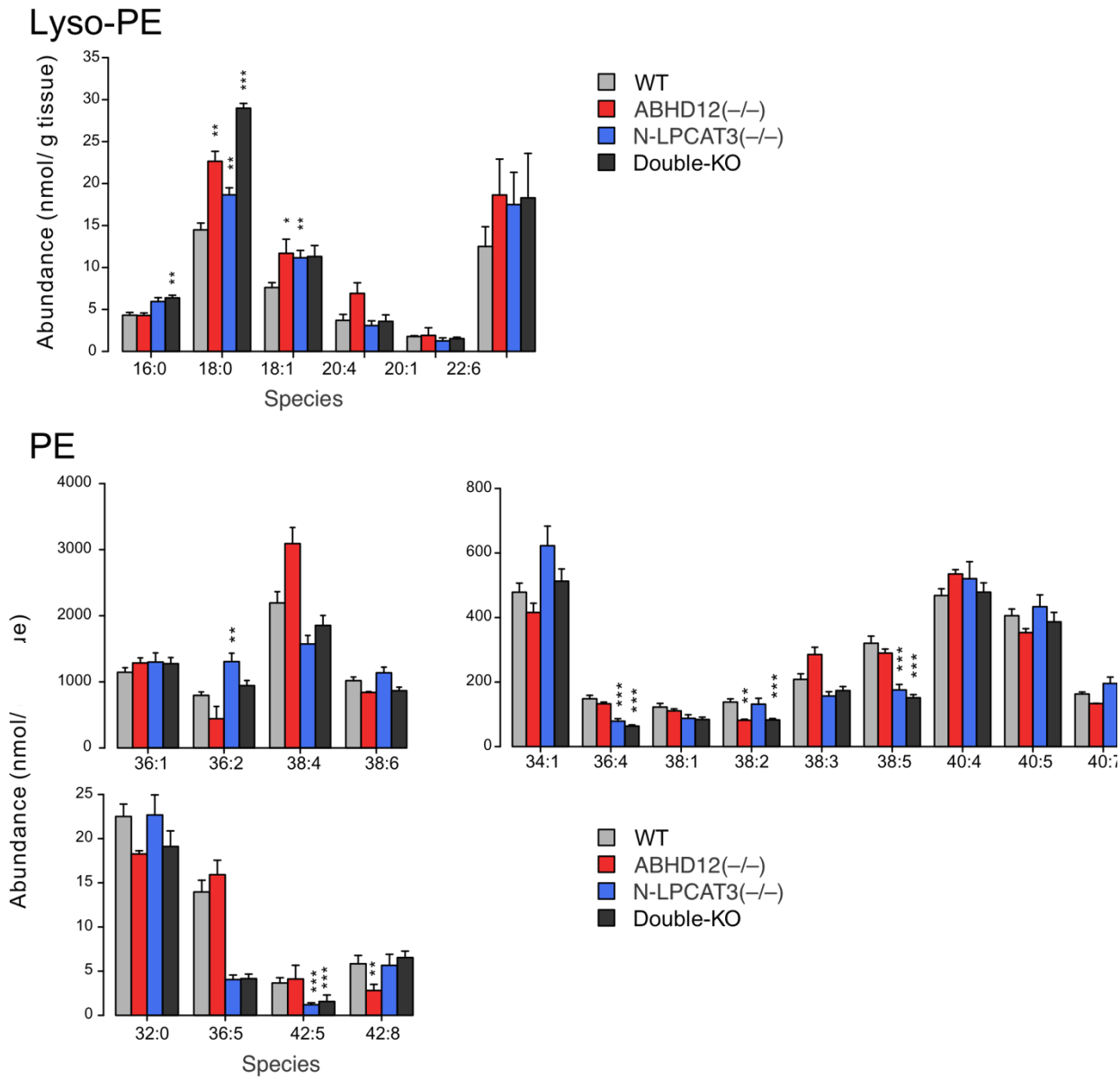

Figure S8. Lyso-PE and PE profiles of 11-week-old ABHD12/N-LPCAT3 double-KO mice. Related to **Figure 3**. Data represent mean ± SE values. n = 5/group. *P < 0.05; **P < 0.01; ***P < 0.001, two-sided Student's t-test performed relative to WT.

Materials and methods

Materials

All chemicals were obtained from Sigma Aldrich unless indicated otherwise. All lipids were purchased from Avanti Polar lipids except for 15:0 FFA (Sigma Aldrich) and 17:1 FFA (Sigma Aldrich). Pharmacological and immunological studies were conducted in C57BL/6 mice. Mice were maintained in pathogen-free conditions and handled in accordance to the requirements of the National Institutes of Health and The Scripps Research Institute Animal Research Committee.

UniProt Accession IDs for human and mouse ABHD12 and LPCAT3

Protein	ID
Human ABHD12	Q8N2K0
Mouse ABHD12	Q99LR1
Human LPCAT3	Q6P1A2
Mouse LPCAT3	Q91V01

Generation of ABHD12/N-LPCAT3 double knockout mice

LPCAT3(fl/fl) were obtained from the Tontonoz laboratory [1] and nestin-Cre mice were obtained from The Jackson Laboratory (JAX stock #003771). ABHD12(+/–)/LPCAT3(fl/fl) and ABHD12(+/–)/LPCAT3(fl/fl) nestin-Cre mice were generated by crossing ABHD12(–/–) mice and LPCAT3(fl/fl) nestin-Cre mice. These mice were further intercrossed to generate ABHD12(–/–)/LPCAT3(fl/fl) nestin-Cre (double-KO) mice. PCR genotyping of genomic tail DNA was performed as previously described [1, 2]. All mice used in this study had *ad libitum* access to water and food.

Lyso-PS hydrolysis assay

The lyso-PS lipase activity of brain membrane lysates from WT, ABHD12(–/–), N-LPCAT3(–/–), and double-KO mice was determined as previously described [3]. Lyso-PS hydrolysis from brain membrane lysates (0.05mg/ml) was determined by the addition of 100 μM 17:1 lyso-PS (20 min, 37 °C). The reaction was quenched with 400 μL of 2:1 $CHCl_3$/MeOH (v/v) with 1 nmol 15:0 FFA as an internal standard. The mixture was vortexed, centrifuged at 1,400 x *g* to separate the aqueous and organic phase. The organic phase was analyzed by LC-MS (1200 LC/MSD, Agilent Technologies). The separation of the analyte was achieved using a 50 mm × 4.6 mm 5 μm Gemini C18 column (Phenomenex) coupled to a guard column (Gemini: C18: 4 × 3 mm). The LC solvents were as follows: buffer A, H_2O:MeOH (95:5, v/v) with 0.1 % NH_4OH (v/v); and buffer B, iPrOH:MeOH:H_2O (60:35:5, v/v/v) with 0.1 % NH_4OH (v/v). The LC method consisted of 0.1 mL/min 20% buffer B for 1.0 min, 0.4 ml/min isocratic mode of 100% buffer B over 7 min and equilibration with 0.5 mL/min 100% buffer A for 3 min. The MS analyses were performed using an electrospray ionization source (ESI) in negative ion mode to measure product formation. MS data were acquired in selected ion monitoring mode at m/z 267.20 for 17:1 FFA and m/z 241.20 for 15:0 FFA.

Lyso-PS acyltransferase assay

Lyso-PS acyltransferase activity of brain membrane lysates from WT, ABHD12(–/–), N-LPCAT3(–/–), and double-KO mice as well as membrane lysates from LPCAT3-deficient THP-1 cells was determined according to the following. Membrane lysates were prepared by sonicating brain lysate or cell pellets in LPCAT3 assay buffer (10mM Tris-HCL (pH 7.4), 1mM EDTA,

0.15M NaCl) using a probe sonicator (Branson Sonifier model 250) with 15 pulses (30 % duty cycle, output setting = 3). Total protein concentrations were determined using the Bio-Rad DC protein assay kit. 50 μM each of 17:1 lyso-PS and 20:4 CoA was added to the membrane lysates (0.05mg/ml) and allowed to incubate for 10 minutes at room temperature. The reaction was quenched by the addition of 2:1 $CHCl_3$/MeOH (v/v) with 1 nmol 17:0/17:0 PS as an internal standard. The mixture was vortexed and centrifuged at 1,400 x *g* to separate the aqueous and organic phase. The organic phase was analyzed by LC/MS–based multiple reaction monitoring (MRM) (Agilent Technologies 6460 Triple Quad). MS analysis was performed using ESI with the following parameters: drying gas temperature, 350 °C; drying gas flow, 9 l/min; nebulizer pressure, 45 Ψ; sheath gas temperature, 375 °C; sheath gas flow, 12 l/min; fragmentor voltage, 100 V; and capillary voltage, 3.5 kV. The separation of the analyte was achieved using a 50 mm × 4.6 mm 5 μm Gemini C18 column (Phenomenex) coupled to a guard column (Gemini: C18: 4 × 3 mm). The LC solvents were as follows: buffer A, H_2O:MeOH (95:5, v/v) with 0.1 % NH_4OH (v/v); and buffer B, iPrOH:MeOH:H_2O (60:35:5, v/v/v) with 0.1 % NH_4OH (v/v). The LC method consisted of 0.8 mL/min 20% buffer B for 6.0 min, 1 ml/min of 100% buffer B over 2 min followed by 20% buffer B for 1 min at 1ml/min and 20% buffer B for 0.50 min at 0.8 ml/min. See Table S1 for MRM transitions.

Metabolomic analysis for cell and brain samples

For cell samples, cells were washed twice with cold DPBS, and the total cell metabolome was extracted in 4 mL 2:1:1 $CHCl_3$/MeOH/DPBS (v/v/v) solution containing the internal standard mix (500 pmol 17:1 FFA, 100 pmol 17:1 lyso-PS, 300 pmol 17:0 lyso-PC, 300 pmol 17:1 lyso-PE, 200 pmol 17:0/20:4 PS, 1 nmol 12:0/12:0 PC and 1 nmol 12:0/12:0 PE. For brain

metabolomic analysis, a half brain was homogenized in a 8 mL glass vial in 4 mL 2:1:1 $CHCl_3$/MeOH/DPBS (v/v/v) solution containing the internal standard mix (1 nmol 17:1 FFA, 500 pmol 17:1 lyso-PS, 5 nmol 17:0 lyso-PC, 5 nmol 17:1 lyso-PE, 400 pmol 17:0/20:4 PS, 10 nmol 12:0/12:0 PC and 10 nmol 12:0/12:0 PE. In both cases, the mixture was vortexed vigorously and centrifuged at 2,000 x *g* for 5 min at 4 °C. The bottom organic phase was collected, and the remaining aqueous phase was acidified with 20 µL (cell samples) or 40 µL (brain samples) formic acid and re-extracted by the addition of 2 mL (cell samples) or 4 mL (brain samples) of $CHCl_3$. Both of the organic phases were pooled, dried down under N_2 gas, and reconstituted in 150 µL (cell samples) or 800 µL (brain samples) 2:1 $CHCl_3$/MeOH (v/v) for LC/MS analysis.

Metabolites analyzed in this study were quantified using LC/MS–based MRM methods (Agilent Technologies 6460 Triple Quad). MS analysis was performed using ESI with the following parameters: drying gas temperature, 350 °C; drying gas flow, 9 l/min; nebulizer pressure, 45 Ψ; sheath gas temperature, 375 °C; sheath gas flow, 12 l/min; fragmentor voltage, 100 V; and capillary voltage, 3.5 kV. The MRM transitions for the targeted LC/MS analysis are presented in Table S1. The separation of metabolites was achieved using a 50 mm × 4.6 mm 5 µm Gemini C18 column (Phenomenex) coupled to a guard column (Gemini: C18: 4 × 3 mm). For negative mode analysis, H_2O:MeOH (95:5, v/v) with 0.1 % NH_4OH (v/v) and iPrOH:MeOH:H_2O (60:35:5, v/v) with 0.1 % NH_4OH (v/v) were used as buffer A and B, respectively. For positive mode analysis, 20 mM ammonium acetate in H_2O and 20 mM ammonium acetate in MeOH were used as buffer A and B, respectively. The LC gradient for negative mode analysis was the following after injection: 20% B at 0.1 mL/min for 5min; then

increase to 85% B at 0.4 mL/min for 15 min; increase to 100% B at 0.5 mL/min for 5 min, run at 100% B at 0.5 mL/min for 2 min; then go back to 20% B and equilibrate at 0.5 mL/min for 5 min. The LC gradient for positive mode analysis was the following after injection: start from 75% B and increase to 99% B at 0.35 mL/min for 22 min; run at 99% B for 17 min; then go back to 75% B and equilibrate for 3 min. Lipid species were quantified by measuring areas under the curve in comparison to the corresponding internal standards and then normalizing to the cell numbers (cell samples) or the wet tissue weight (brain samples).

Generation of CRISPR-mediated LPCAT3-deficient THP-1 cells

LPCAT3-deficient THP-1 cells were generated according to a previously described previously[4]. Lentiviral shRNAs targeting the messenger RNA for human LPCAT3 and a control shRNA were cloned into pLKO.1 vector at the Age1, EcoR1 sites as described previously[5]. The sequences for these shRNAs is described below (sequences are 5' to 3').

sgCTRL1-fwd:caccGAACCTACGGGCTACGATACG

sgCTRL1-rev:aaacCGTATCGTAGCCCGTAGGTTC

sgLPCAT3-1-fwd:caccGAGACTCAGGCGCTTGAGAGC

sgLPCAT3-1-rev:aaacGCTCTCAAGCGCCTGAGTCTC

sgLPCAT3-2-fwd:caccGACTGAAGCACAATACACAGC

sgLPCAT3-2-rev:aaacGCTGTGTATTGTGCTTCAGTC

sgLPCAT3-3-fwd:caccGTCACGTCATAGTCTTCAGTG

sgLPCAT3-3-rev:aaacCACTGAAGACTATGACGTGAC

shRNA-encoding plasmids were co-transfected with DVPR envelope and CMV VSV-G packaging plasmids into 2.5x10^6 HEK293T cells using the Xtremegene 9 transfection reagent (Sigma-Aldrich). Virus-containing supernatants were collected 48 h after transfection and used to infect target THP-1 cells. For the THP-1 cell infection, 0.25x10^6 THP-1 cells were plated in a 6-well plate in 1 mL of media followed by the addition of 1 mL of virus-containing supernatant for each sgRNA to the respective wells and 10ug/mL of polybrene (Sigma-Aldrich). The 6-well plate was centrifuged at 300 x g for 2 hours at 30 ºC. Following the centrifugation, cells were collected into 15 mL conical tubes, centrifuged at 500 x g for 3 min at room temperature, media was aspirated, and the cells were transferred to a new 6-well dish in 4 mL of media. The cells were allowed to recover for 48 h and puromycin (2 µg/mL) was added to the cells. To select for puromycin-resistant cells, the cells were grown at a density between 0.4 x 10^6 and 0.8 x 10^6 cells/ml to avoid high density and the media was continually replenished for two weeks to remove dead cells. Puromycin-resistant cells were expanded and analyzed for lyso-PS acyltransferase activity.

Synthego ICE Analyses of LPCAT3-null THP-1 cells

CRISPR editing efficiency was assessed using the Synthego ICE analysis software (https://ice.synthego.com). Genomic DNA was isolated from sgCtrl- and sgLPCAT3- treated THP-1 cells using the PureLink Genomic DNA Mini Kit (ThermoFisher Scientific) and PCR amplified using the following primers for each LPCAT3 CRISPR-Cas9 cut site:

LPCAT3-1-F: GAAACAGGAAACACTTTGGGCAGC

LPCAT3-1-R: TATCTGTAGGGATCCTTGCCTG

LPCAT3-3-F: GAAACAGGAAACACTTTGGGCAGC

LPCAT3-3-R: GCTGGCATTGACAACTCACAGATCT

Samples were PCR purified and subjected to Sanger sequencing using the above primers. The sequencing ab1 files were uploaded to the Synthego ICE software for analysis.

In situ treatment of LPCAT3-deficient THP-1 cells with DO264

LPCAT3-deficient THP-1 cells were grown and maintained in RPMI 1640 media (ThermoFisher Scientific) containing 10 % (v/v) FBS (Omega Scientific), 2 mM L-glutamine, 100 U/mL penicillin-streptomycin (GE Life Sciences), and 0.05 mM 2-mercaptoethanol at 37 °C with 5 % CO_2. For *in situ* treatment of THP-1 cells with DO264, 6 million cells were cultured in 10 mL media in the presence of DMSO or DO264 (1 μM) for 4 h at 37 °C with 5 % CO_2. After the incubation, the cells were washed twice with ice-cold DPBS and stored at -80 °C for metabolomic analyses.

Compound treatment for _in vivo_ studies

For oral gavage (p.o.), DO264 was resuspended in 20% (2-hydroxypropyl)-β-cyclodextrin in H_2O (v/v) by probe and bath sonication. 10 μL/g mouse body weight of the freshly prepared compound solution was administered by oral gavage. Compound-treated mice were anesthetized

with isoflurane and euthanized by cervical dislocation to harvest tissues. The experiments were conducted in accordance with the guidelines of the Institutional Animal Care and Use Committee of The Scripps Research Institute.

Auditory startle test

Auditory startle response testing was performed using SR-Lab startle chambers (San Diego Instruments). Acoustic stimuli were produced by high-frequency speakers controlled by SR-Lab software. A 25-min test session was used, in which pulse values were 90, 95, 100, 105, 110, 115, and 120 dB on a 70-dB background level. Startle pulses were 40 ms in duration and the trial types were presented 6-10 times in a pseudorandom order with intervening no stimulus trials to control for baseline movement. Data are presented as the average startle magnitude measured during each acoustic pulse ± SEM. As a control experiment, auditory startle response test was performed on aged WT and nestin-Cre mice, and there was no significant difference in startle response between WT and nestin-Cre mice.

Iba1 staining of micrgolia in the cerebellum

Mice were deeply anesthetized using isoflurane and perfused with 0.1 M phosphate buffer (PB), followed by 4% (w/v) paraformaldehyde. Perfused brains were post-fixed in 4% paraformaldehyde overnight, cryoprotected in 30% (w/v) sucrose in 4% paraformaldehyde until they sank (~3 d), and rapidly frozen on dry ice. Coronal 25-μm sections were cut on a Leica CM1850 cryostat. Immunohistochemistry was performed on frozen, free-floating cryostat sections (25 μm). Sections from 12-month-old WT, ABHD12(–/–), N-LPCAT3(–/–), and double-KO mice (n = 4) were immunostained with anti-Iba1 antibody (1/500 dilution; Wako,

019-19741). Sections were incubated with primary antibodies in 0.5% (w/v) BSA in 0.1 M PB for 48 h at 4 °C, incubated with secondary antibody (anti–rabbit-biotin; Vector Laboratories, BA-1000-1.5; 1/300 dilution of 1.5 mg/mL stock) in 0.5% (w/v) BSA in 0.1 M PB for 1 h at room temperature and detected with ABC Elite Vectastain (Vector Laboratories) for 1 h. Diaminobenzidine (DAB) (peroxidase substrate kit; Vector Laboratories) was used as the chromogen. Sections were washed in 0.1 M PB after staining and mounted in VectaMount. Immunostained sections were imaged using a Leica SCN400 whole slide scanner. Quantitation of Iba1-positive, enlarged microglia (>200 μm^2) was performed in the cerebellar region depicted by the black box in Figure 4B in five matching cerebellar sections per mouse using ImageJ software (National Institutes of Health).

Statistics

Statistical analyses were performed using the R statistical programming language. All data are shown as mean values ± SEM and two-sided Student's *t*-test was used to perform statistical analyses. The following criteria were used to indicate statistical significance: * $p < 0.05$ with a fold change greater than 1.5 or lower than 0.67; ** $p < 0.01$; and *** $p < 0.001$.

References

[1] Rong, X., Wang, B., Dunham, M. M., Hedde, P. N., Wong, J. S., Gratton, E., Young, S. G., Ford, D. A., and Tontonoz, P. (2015) Lpcat3-dependent production of arachidonoyl phospholipids is a key determinant of triglyceride secretion, *Elife 4*.

[2] Blankman, J. L., Long, J. Z., Trauger, S. A., Siuzdak, G., and Cravatt, B. F. (2013) ABHD12 controls brain lysophosphatidylserine pathways that are deregulated in a murine model of the neurodegenerative disease PHARC, *Proc Natl Acad Sci U S A 110*, 1500-1505.

[3] Ogasawara, D., Ichu, T. A., Vartabedian, V. F., Benthuysen, J., Jing, H., Reed, A., Ulanovskaya, O. A., Hulce, J. J., Roberts, A., Brown, S., Rosen, H., Teijaro, J. R., and Cravatt, B. F. (2018) Selective blockade of the lyso-PS lipase ABHD12 stimulates immune responses in vivo, *Nat Chem Biol 14*, 1099-1108.

[4] Shalem, O., Sanjana, N. E., Hartenian, E., Shi, X., Scott, D. A., Mikkelson, T., Heckl, D., Ebert, B. L., Root, D. E., Doench, J. G., and Zhang, F. (2014) Genome-scale CRISPR-Cas9 knockout screening in human cells, *Science 343*, 84-87.

[5] Sarbassov, D. D., Ali, S. M., Kim, D. H., Guertin, D. A., Latek, R. R., Erdjument-Bromage, H., Tempst, P., and Sabatini, D. M. (2004) Rictor, a novel binding partner of mTOR, defines a rapamycin-insensitive and raptor-independent pathway that regulates the cytoskeleton, *Curr Biol 14*, 1296-1302.